PROCEEDINGS, Twentieth Workshop on Geothermal Reservoir Engineering
Stanford University, Stanford, California, January 24-26 1995
SGP-TR-150

INTERPRETATION OF PRE- AND POST-FRACTURING WELL TESTS IN A GEOTHERMAL RESERVOIR

Norio Arihara[1], Hiroshi Fukagawa[1], Masami Hyodo[2] and Maghsood Abbaszadeh[3]

1. Waseda University, Tokyo 169, Japan
2. Geothermal Energy Research and Development Co., Ltd, Tokyo 103, Japan
3. Japan National Oil Corporation, Chiba 260, Japan

ABSTRACT

Pre- and post-fracturing well tests in TG-2 well drilled next to the Matsukawa field are interpreted for evaluating effects of a massive hydraulic fracturing treatment. The interpreted data include multiple-step rate tests, a two-step rate test, and falloff tests. Pressure behaviors of massive hydraulic fracturing are matched by a simulator of dynamic fracture option.

Fracture parting pressures can be evaluated from the multiple-step rate test data. The multiple-step rates during the massive hydraulic fracturing treatment show that multiple fractures have been induced in sequence. Although the pre-fracturing falloff tests are too short, fracture propagation can be evaluated qualitatively from the falloff data. Interpretation of the falloff test immediately after the MHF suggests that extensive fractures have benn created by the MHF, which is verified by simulation. The post-fracturing falloff tests show that the fractures created by the MHF have closed to a great degree.

INTRODUCTION

Hydraulic fracturing is an effective way of well stimulation in tight oil and gas reservoirs. Development of geothermal systems including hot dry rock reservoirs also employs this technology (Wright et al., Tester et al.). Design and evaluation of a field operation of hydraulic fracturing are important and difficult tasks particularly for geothermal reservoirs, because fluid flow is predominantly controlled by natural fractures.

Well testing either by producing or by injecting fluid is normally conducted before and after hydraulic fracturing in order to obtain data for reservoir evaluation. Injection and falloff tests in water injection wells are common practices of the pressure transient test in oil fields under waterflooding. Analysis of injection and falloff tests can be complicated by two important effects: the multiphase effect and temperature effect.

If the injected fluid is different from the reservoir fluid, a saturation front propagates into the reservoir, and a saturation gradient is established in the reservoir because of differences in fluid properties. In case of water injection into an oil reservoir at the connate stage, the oil bank with initial water saturation is located ahead of the injection front. Abbaszadeh and Kamal (1989) presented an interpretation method for injectivity and falloff testing considering saturation gradients. They prepared type curves for falloff tests.

In a water injection well test, the injected fluid usually has a temperature different from the initial reservoir temperature. A temperature front also propagates into the reservoir. As viscosity is a temperature-dependent parameter, the well test interpretation has to account for this effect. Bratvold and Horne (1990) presented generalized procedures to interpret pressure injection and falloff data following cold-water injection into a hot oil reservoir. They showed that type-curve matching provides estimates of parameters such as the temperature-dependent mobilities of the flooded and uninvaded regions, the size of the invaded region, and the distance to the temperature discontinuity.

Another complexity in injection and falloff tests is caused by dynamic fractures. Several authors reported on pressure transient analysis for fractured water injection wells. Larsen and Bratvold (1994) analysed effects of propagating fractures on pressure-transient injection and falloff data. They modified the previous solutions of the cold-water injection and falloff (Bratvold and Horne) to cover flow in elliptic systems and to account for the propagating fracture. By matching pressure-transient data and analytical solutions, key parameters such as fracture propagation, reservoir and fluid parameters, and temperature and saturation profiles can be determined.

In well testing at geothermal reservoirs, the temperature of a injected fluid can be much lower than the reservoir temperature. As a possible injection rate is quite high in geothermal well testing, dynamic fractures also can be easily induced being initiated from natural fractures.

The principal objectives of this paper are to interpret pre- and post-fracturing well tests, and to evaluate physical mechanisms of hydraulic fracturing in a geothermal reservoir.

DISCUSSIONS

Background

The tested well TG-2 was drilled next to the Matsukawa geothermal field under a plan to produce steam after creating communication with the Matsukawa reservoir by hydraulic fracturing. This was a part of the "Technology for Increasing Geothermal Energy Recovery" project of the New Energy and Industrial Technology Development Organization. The well is deviated and of the open hole interval 710 - 1,298 m depth. The target zone for hydraulic fracturing consists mainly of naturally fractured silt and tuff formations (Shinohara and Takasugi). Mutiple-step rate tests by fresh water and injection tests by different gels were first carried out to choose an injection fluid and to evaluate reservoir properties for hydraulic fracturing.

After having decided to use fresh water for testing and fracturing, pre-fracturing well tests, a massive hydraulic fracturing (MHF) treatment, and post-fracturing well tests were performed sequentially. All the well tests accomplished were injection and falloff tests. In all the tests except the multi-step rate and gel injection tests, and the MHF, production logging was run to survey injection profiles, and pressure and temperature gradients during the injection period, and then the tool was stationed at a fixed depth to monitor falloff pressures (Ujo et al.).

Test Procedure

Testing and operation consist of four parts:

(1) Two multiple step rate tests (MSRT-1, and MSRT-2) with fresh water and three gel injection tests, conducted on January 23 through 26, 1992, to choose a fracturing fluid and to evaluate formation properties;

Pressure and rate data of MSRT-1 and MSRT-2 are shown in Fig. 1. In MSRT-1, the rate was increased by ten steps from 0 to 12 BPM for 54.5 minutes. In MSRT-2, the rate was increased by nine steps from 0 to 16 BPM for 50.0 minutes. Three gel injection tests were performed with YF-650, YF-660 and PSS polymers respectively, each at about 10 BPM for about 50 minutes.

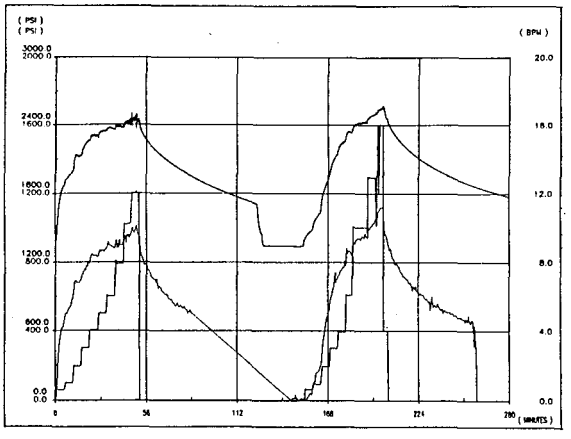

Fig. 1 - Multiple-step rate tests MSRT-1 and -2 and falloff tests

(2) Two injection-falloff tests with fresh water conducted in sequence on September 22, 1992, to evaluate pre-frac properties of formation;

As shown in Fig. 2, the first injection (IT-1) continued at about 0.88 BPM (1261 BPD) for 48 min. and was followed by a falloff test FOT-1. The second injection test (IT-2) was at about 9.42 BPM (13562 BPD) for 75 min. and a longer falloff test (FOT-2) followed immediately after injection.

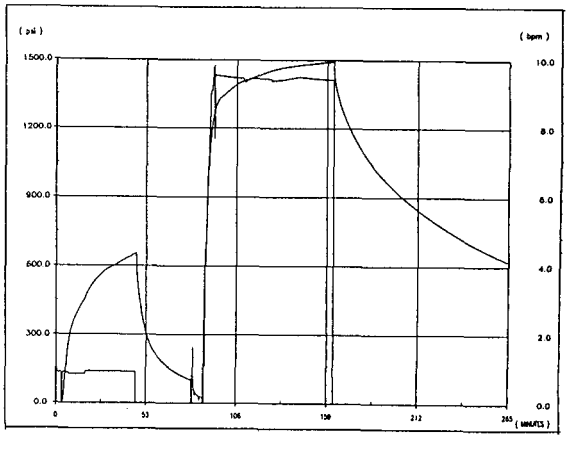

Fig. 2 - Two-step rate tests

(3) MHF operated with fresh water on November 24 and 25, 1992 (Hyodo et al., Wright et al.);

Pressure and rate records are shown in Fig. 3. The injection rate was initially increased stepwise to a maximum rate 25.4 BPM and kept between 25.4 and 24.5 BPM. Injection was interrupted four times, each time for about 30 min. Total injected water amounts to 27,400 Bbls. A pressure falloff test followed 24 hours injection.

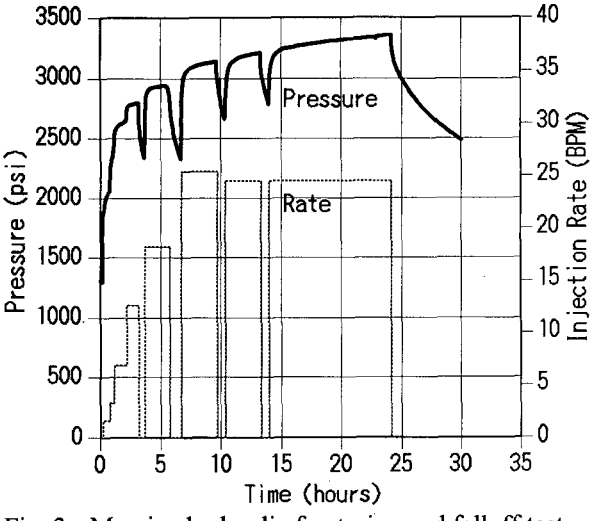

Fig. 3 - Massive hydraulic fracturing and falloff test

(4) Two post-frac injection-falloff tests conducted on November 27 and 29, 1992, respectively;
Fresh water was injected at a rate of 9.44 BPM for 4.14 hours and 1.87 hours before the November 27 falloff test (FOT-3) and the November 29 falloff test (FOT-4), respectively.

Analysis of Step Rate Tests

Bottom-hole flowing pressures of MSRT-1 and MSRT-2 are graphed against injection rate as shown in Fig. 4. The plotted pressures are taken at the end of each rate step. Fig. 4 shows that linear increases in pressure break twice at about 2,000 and 2,250 psia in both tests as injection rate increases. A fracture started parting at 2,000 psia and another fracture was induced at 2,250 psia, and both kept propagating above 2,250 psia.

Fig. 5 shows also bottom-hole flowing pressures vs. injection rate for the first five step rates of the MHF. Although conclusive interpretation is not allowed because of scarce data points, the pressure does not break sharply but gradually bend between about 2,200 and 2,700 psia. This suggests that multiple fractures were induced sequentially. Another observation is that the parting and propagating pressures are much higher than those of MSRT-1 and MSRT-2, which

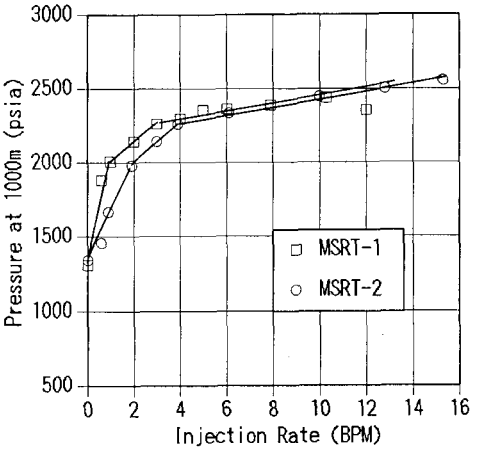

Fig. 4 - Pressure vs. rate plot for step rate analysis

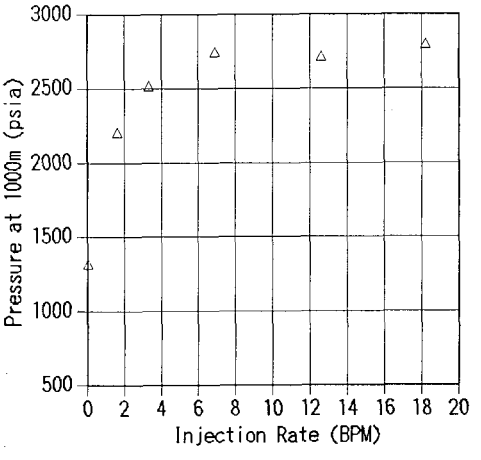

Fig. 5 - Pressure vs. rate plot for step rate analysis

means that the fractures created by the MHF propagate into zones of different rock properties.

Injection pressures of IT-1 and IT-2 are interpreted by the method proposed by Singh and Agarwal (1990). Figs. 6 and 7 plot the pressure function $\Delta p/\Delta q$ against the multirate equivalent time assuming radial flow and linear flow, respectively, where $\Delta p = p_{wf_n}(\Delta t) - p_{wf_{n-1}}(t_{n-1})$ and $\Delta q = q_{n-1} - q_n$. Here, pressures of IT-1 are well below an estimated fracture parting pressure, and therefore can be taken as the baseline data. Data for the two steps coincide as long as the fracture parting pressure (FPP) is not exceeded. When the FPP is exceeded during the second step IT-2, the IT-2 data beyond this time will deviate from the baseline IT-1 data with a smaller slope. From Figs. 6 and 7, the FPP is estimated to be 2,038 psia at an equivalent time of about 0.014 hours.

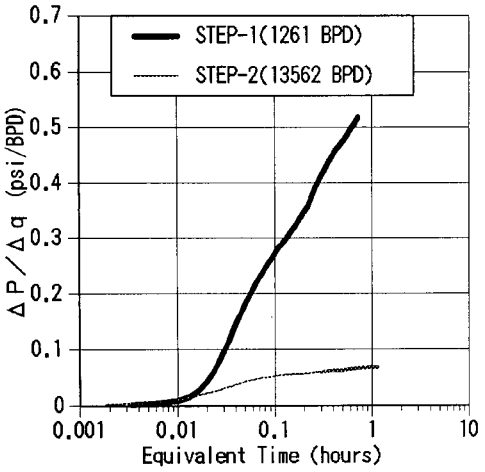

Fig. 6 - Radial-flow multirate equivalent-time analysis for 2-step rate test

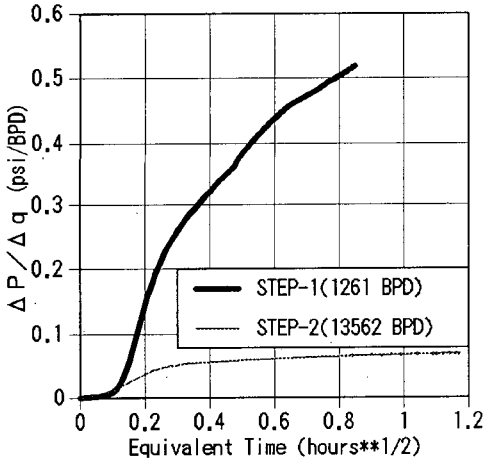

Fig. 7 - Linear-flow multirate equivalent-time analysis for 2-step rate test

Analysis of Pre-Fracturing Falloff Tests

The falloff tests after MSRT-1 and MSRT-2, and falloff tests FOT-1 and FOT-2 were interpreted without considering effects of propagating fractures. As the multiple-step rate tests MSRT-1 and MSRT-2, and the injection test IT-2 definitely reflect fracture propagation, meaningful interpretation is to be attempted by an appropriate method (Larsen and Bratvold).

All the pre-frac falloff data turned out to be too short to obtain full reservoir information. Figs. 8 and 9 are the pressure and derivative plots of the falloff tests after MSRT-1 and MSRT-2, respectively. The falloff test after MSRT-1 shows only a behavior of linear flow into infinite conductivity fracture. Effective (or equivalent) fracture half-length x_f can be estimated

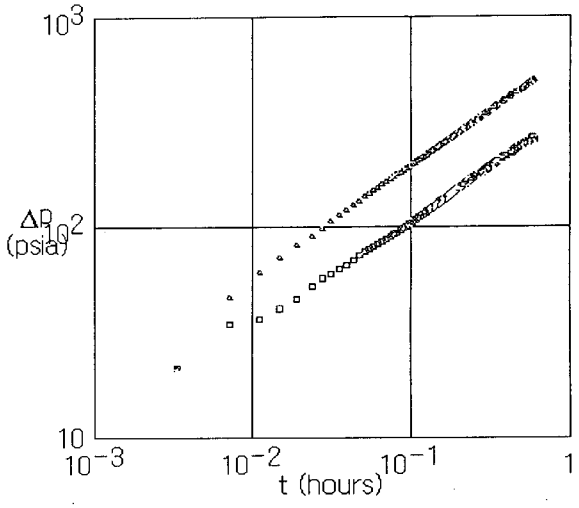

Fig. 8 - Log-log plot of falloff data after MSRT-1

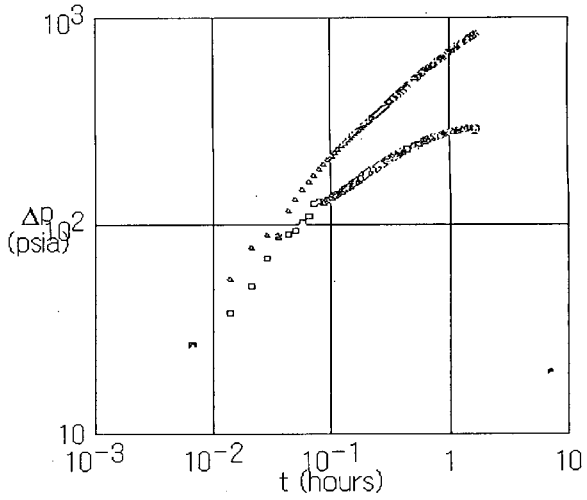

Fig. 9 - Log-log plot of falloff data after MSRT-2

from the slope of pressure vs. $\sqrt{t}$ plot, knowing permeability-thickness product kh of formation. Estimating a kh value is not correctly done, however, as the duration of the falloff time is too short to obtain radial flow information. The falloff test after MSRT-2 shows a fractured well behavior as indicated by the half slope on the derivative curve. This has a longer duration, but has not reached radial flow either as seen in Fig. 9. $x_f h^{1/2}$ is evaluated to be 1,840 $ft^{3/2}$ if a kh value 725 md·ft calculated by the last part of the data is used.

FOT-1 and FOT-2 are plotted as Figs. 10 and 11, respectively. FOT-1 has not quite reached radial flow yet, but is slowly approaching there. Thus an

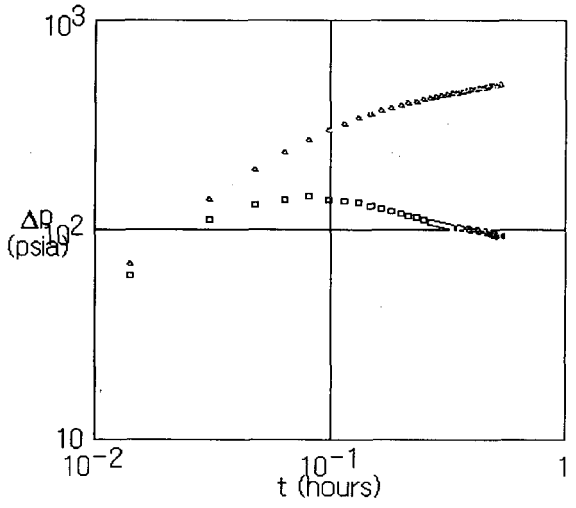

Fig. 10 - Log-log plot of falloff test FOT-1

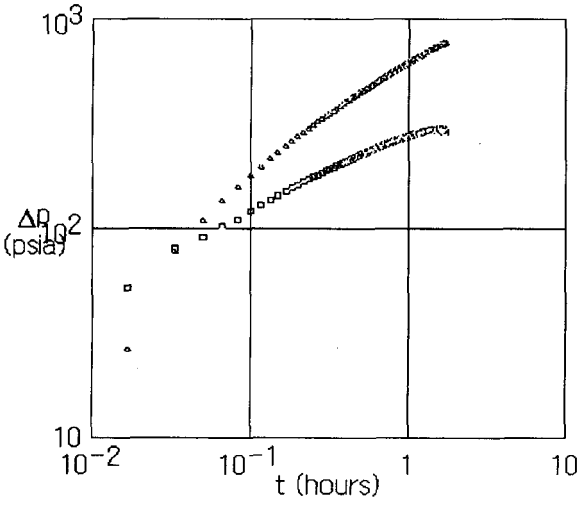

Fig. 11 - Log-log plot of falloff test FOT-2

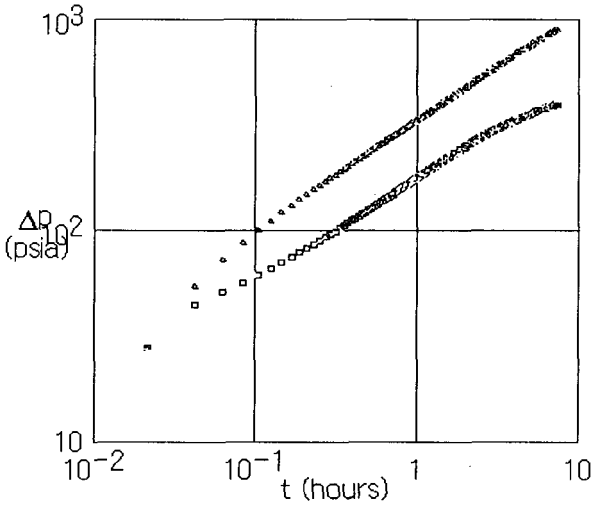

Fig. 12 - Log-log plot of falloff data following MHF

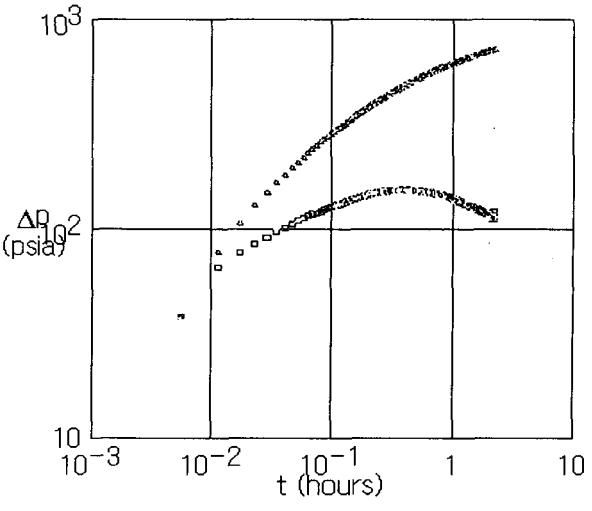

Fig. 13 - Log-log plot of falloff test FOT-3

estimated kh value 122 md·ft is considered to be the lower bound. This low kh value may represent a small net thickness h before fracturing as testing pressures are lower than the fracture parting pressure. FOT-2 is similar to the falloff test after MSRT-2. $x_f h^{1/2}$ is calculated as 1,750 $ft^{3/2}$ with a kh of 430 md·ft estimated from the slope of the last portion of the data.

Analysis of Post-Fracturing Falloff Tests

The falloff test immediately after the MHF clearly shows a behavior of infinite conductivity fracture as seen in Fig. 12. All the pressure data are still in the linear flow region and radial flow has not been reached yet. If the kh value 430 md·ft obtained by FOT-2 is assumed, an effective value of $x_f h^{1/2}$ is estimated to be 8,380 $ft^{3/2}$ which proves that extensive fracturing has been accomplished.

Fig. 13 shows the falloff test FOT-3 on November 27, two days after the MHF. Figs. 14 and 15 plot the falloff test FOT-4 on November 29, four days after the MHF. These two tests show very similar transient behaviors such that FOT-3 is shorter and only an early part of FOT-4. These plots seem to indicate two zone behavior by two constant derivatives, the inner zone with a lower kh and the outer zone with a higher kh. It is not clearly understood what causes the inner zone, but the outer zone properties dominate the late radial flow from which kh is estimated as 2,045 md·ft. Using this kh value and the slope of pressure vs. $\sqrt{t}$

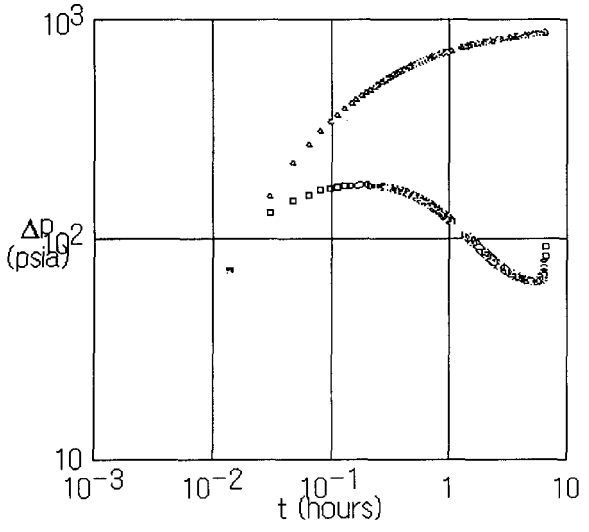

Fig. 14 - Log-log plot of falloff test FOT-4

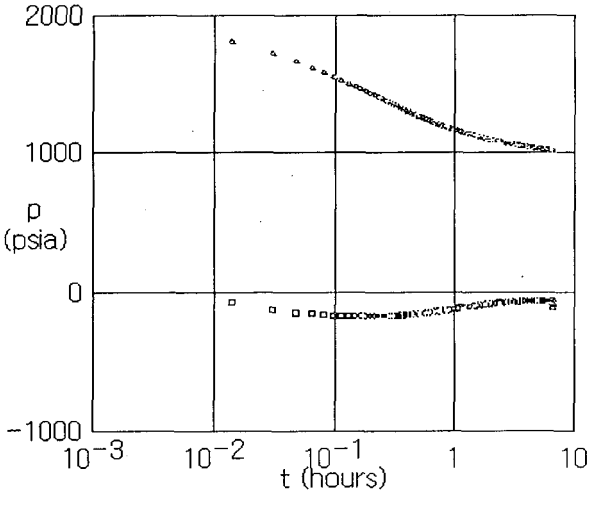

Fig. 15 - Semi-log plot of falloff test FOT-4

plot, $x_f h^{1/2}$ is estimated to be 390 $ft^{3/2}$. The high kh value may most likely be caused by the fact that network of fractures has extended both vertically and laterally, giving an effectively large thickness h to the system. The injection profiles measured by production logging before and after the MHF support this interpretation (Shinohara and Takasugi). The effective fracture half-length has decreased remarkably, however, which proves that the initial goal of establishing communication with the Matsukawa reservoir cannot be achieved.

Simulation of MSRT-1 and MHF

MSRT-1 including the pressure falloff immediately

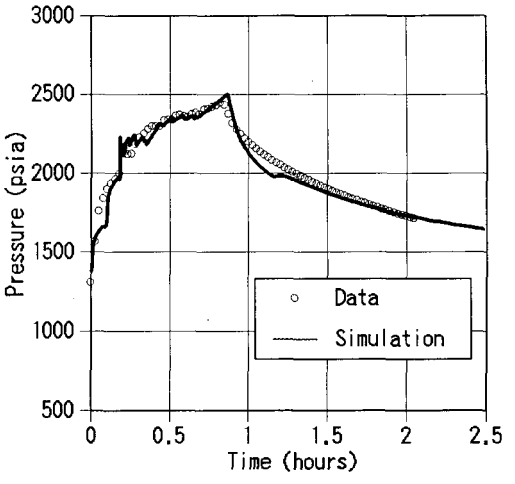

Fig. 16 - Simulation of MSRT-1 and falloff data

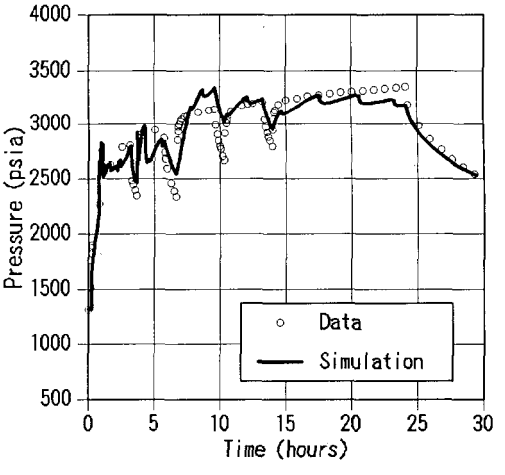

Fig. 17 - Simulation of MHF and falloff data

after it and the MHF have been simulated by STARS, a thermal oil recovery simulator which has a dynamic fracture option. This option was enabled essentially by four parameters; (a) fracture opening pressure, (b) a range of pressure over which fracture opens, (c) maximum transmissibility multiplier to be applied for fully open fracture, and (d) location of fracture.

Fig. 16 is a matching result by a 2D areal model for which the parameter values as shown in Table 1 were used. The gradual increase in pressure during injection could be reasonably matched by assuming that the well rows and columns are dynamically fractured up to 80 feet away from the well. Formation permeability is assumed to be 0.9 md except the row blocks dynamically fractured are assigned 5 md initially.

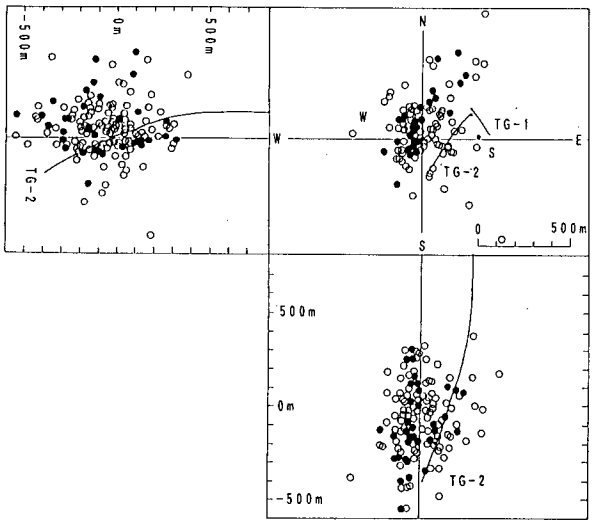

Fig. 18 - Epicenter plot of AE events during MHF (• : AE of S/N bigger than 45dB)

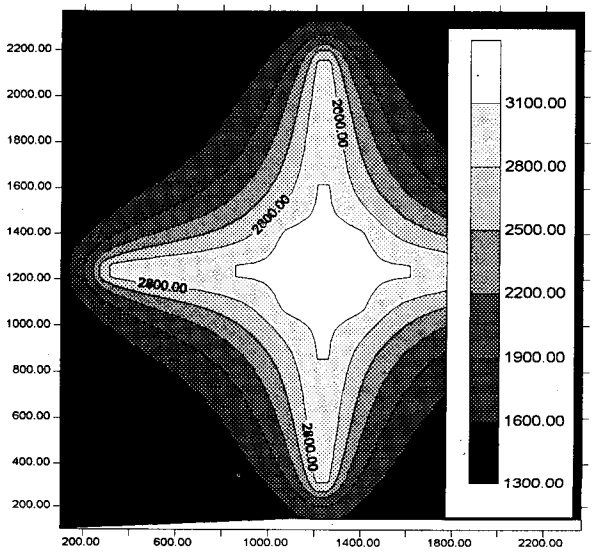

Fig. 19 - Simulated pressure distribution at the end of MHF

Simulation of the MHF was also made by a 2D areal model of the parameters as shown in Table 1. In order to reproduce the pressure behavior as shown in Fig. 17, extensive dynamic fracturing needs to be assumed, i.e. areal propagation for the 410 ft x 410 ft square zone with the well at center as well as linear propagation along the well rows and columns up to 980 ft away from the well. Fig. 18 shows the acoustic emission recorded during the MHF, which can be referred to for qualitative verification of the geometry

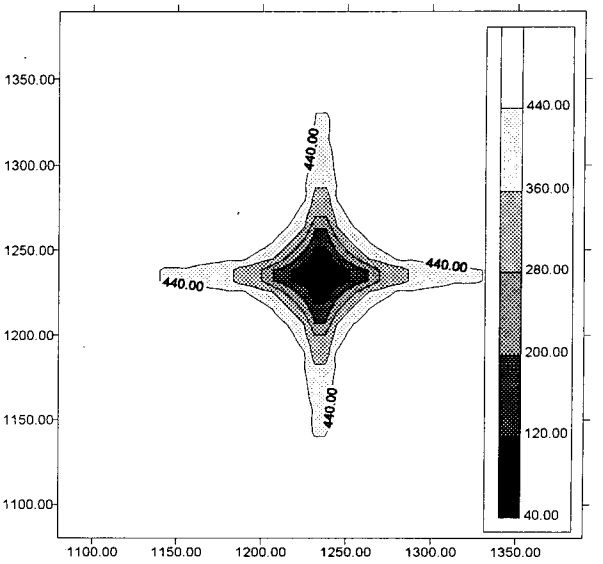

Fig. 20 - Simulated temperature distribution at the end of MHF

	MSRT-1 model	MHF model
Matrix porosity	0.1	0.1
Matrix perm., md	two 80' rows: 5. others: 0.9	two 980' rows, col's: 20. others: 0.9
Frac open press., psi	2,000	2,500
Press. range to full open frac	100	100
Max frac trans. multiplier	10,000	10,000
Frac location	two 80' rows & columns	two 980' rows & col's, 410'x410' area

Table 1 - Parameters for dynamic fracture simulation

and dimension of fracture propagation. As seen in the planview plot, the acoustic emission events are dense within about 200 m distance from the well. Figs. 19 and 20 shows the simulated pressure and temperature distributions at the end of the MHF injection.

CONCLUSIONS

1. Two values of the fracture parting pressure (FPP) can be detected from the multiple-step rate test data. The multiple-step rates during the massive hydraulic fracturing treatment also show multiple FPP's.
2. The pre-fracturing falloff tests are too short in time

to obtain the true formation kh. Evaluation of $x_f h^{1/2}$ may be possible from the falloff data, however, by assuming a kh calculated from the last part of the falloff data.

3. Interpretation of the falloff test immediately after the MHF gives a large effective value of $x_f h^{1/2}$ which suggests that extensive fractures have been created by the MHF. Simulation of the MHF also requires an extensive three-dimensional fracture network to reproduce the observed pressure behavior.

4. The post-fracturing falloff tests show that the fractures created by the MHF have closed to a great degree.

ACKOWLEDGMENTS

The field data and information used in this study were obtained in the "Technology for Increasing Geothermal Energy Recovery" project of the New Energy and Industrial Technology Development Organization (NEDO). The authors would like to thank NEDO for permission to present this paper.

Well test analysis was accomplished by AutoWIN, the well test interpretation system developed by Petroway, Inc. in Palo Alto, California.

The simulation model used is STARS developed by Computer Modelling Group in Calgary, Canada.

REFERENCES

1. Abbaszadeh, M. and Kamal, M.: "Pressure-Transient Testing of Water-Injection Wells", *SPE Reservoir Engineering*, (Feb. 1989), 115-124.

2. Bratvold, R.B. and Horne, R.N.: "Analysis of Pressure-Falloff Tests Following Cold-Water Injection", *SPE Formation Evaluation*, (Sept. 1990), 293-302.

3. Hyodo, M., Shinohara, N. and Takasugi, S.: "Hydraulic Fracturing Test and Pressure Behavior Analysis at the TG-2 Well", Preprints, SEG Japan, June 1993.

4. Koning, E.J.L. and Niko, H.: "Fractured Water-Injection Wells: A Pressure Falloff Test for Determining Fracture Dimensions", paper *SPE 14458* presented at the 1985 SPE Annual Technical Conference and Exhibition, Las Vegas, Sept. 22-25.

5. Larsen, L. and Bratvold, R.B.: "Effects of Propagating Fractures on Pressure-Transient Injection and falloff Data", *SPE Formation Evaluation*, (June 1994), 105-114.

6. Peng, C.P., Singh, P.K., Halvorsen, H. and York, S.D.: "Fractured Reservoir Characterization Through Injection, Falloff, and Flowback Tests", *SPE Formation Evaluation*, (Sep. 1992), 241-246.

7. Shinohara, N. and Takasugi, S.: "Fracture Design and the Result of Mini Hydraulic Fracturing, Employed for the TIGER Project", Preprints, SEG Japan, June 1993.

8. Singh, P. and Agarwal, R.G.: "Two-Step Rate Test: New Procedure for Determining Formation Parting Pressure", *J. Pet. Eng.*, (Jan. 1990), 84-90.

9. Tateno, M., Wei, Q. and Hanano, M.: "Evaluation of Fracture Extension Created by Hydraulic Fracturing using AE measurement, employed for TIGER Project", Preprints, SEG Japan, June 1993.

10. Tester, J.W., Murphy, H.D., Grigsby, C.O., Potter, R.M. and Robinson, B.A.: "Fractured Geothermal Reservoir Growth Induced by Heat Extraction", *SPE Reservoir Engineering*, (Feb. 1989), 97-104.

11. Ujo, S., Shinohara, N. and Takasugi, S.: "Evaluation of Productivity Improvement by Hydraulic Fracturing Using PTS Logging at the TG-2 Well", Preprints, SEG Japan, June 1993.

12. Wright, C.A., Tanigawa, J.J., Hyodo, M. and Takasugi, S.: "Real-Time and Post-Frac' #-D Analysis of Hydraulic Fracture Treatments in Geothermal Reservoirs", Preprints, Nineteenth Annual Workshop Geothermal Reservoir Engineering, January 1994.